Development 127, 3197-3204 (2000)
Printed in Great Britain © The Company of Biologists Limited 2000
DEV0299



# A series of novel mutants of *Arabidopsis thaliana* that are defective in the formation of continuous vascular network: calling the auxin signal flow canalization hypothesis into question

**Koji Koizumi[1,*], Munetaka Sugiyama[2] and Hiroo Fukuda[1]**

[1]Department of Biological Sciences, Graduate School of Science, The University of Tokyo, Hongo 7-3-1, Bunkyo-ku, Tokyo 113-0033, Japan
[2]Botanical Gardens, Graduate School of Science, The University of Tokyo, Hakusan 3-7-1, Bunkyo-ku, Tokyo 112-0001, Japan
*Author for correspondence (e-mail: ss77213@mail.ecc.u-tokyo.ac.jp)

*Accepted 8 May; published on WWW 10 July 2000*

## SUMMARY

**For the genetic analysis of molecular mechanisms underlying temporal and spatial regulation of vascular pattern formation, we isolated mutants of *Arabidopsis thaliana* that are impaired in vascular patterning. Microscopic examination of the cotyledonary venation of 3,400 $M_3$ lines led to the identification of 12 mutant lines. Genetic analysis of 8 of these mutant lines indicated that vein pattern formation in these lines resulted from monogenic recessive mutations in 7 different genes, designated *VAN1* through *VAN7*. Mutations in *VAN1* through *VAN6* genes caused fragmentation (disconnection or partial loss) of lateral veins of the cotyledon and tertiary veins of the rosette leaf whereas they were less injurious to the formation of major veins. Detailed characterization of the *van3* mutant using *pAthb8::GUS* and *pTED3::GUS*, as molecular markers for the early stage of vascular tissue formation showed that the provascular tissue of the cotyledonary lateral veins was differentiated in fragments during late embryogenesis. These phenotypes of the *van* mutants are discussed in relation to the auxin signal flow canalization hypothesis and the diffusion-reaction prepattern hypothesis, with the fragility of the continuity in the minor vein formation favoring the latter hypothesis.**

Key words: *Arabidopsis thaliana*, Auxin signal flow canalization hypothesis, Cotyledon, Diffusion-reaction prepattern hypothesis, Provascular tissue, Vascular network, Venation, *VAN*

## INTRODUCTION

The construction of vascular systems during organ development has provided a model for studying pattern formation as well as tissue differentiation in plants. One can recognize a rich variety of patterns in vascular systems among different species and organs. Despite such diversity in the apparent vascular patterns, it has been thought that a common basic mechanism underlies spatial regulation of vascular tissue formation. With respect to this supposed mechanism, two noteworthy hypotheses have been proposed up to now. One is the auxin signal flow canalization hypothesis (Sachs, 1989, 1991), which is based primarily on experimental observation of the inductive effect of auxin on vascular tissue formation, and the other is the diffusion-reaction prepattern hypothesis (Meinhardt, 1982; Koch and Meinhardt, 1994), which is based on computer modeling of interactions among hypothetical diffusible substances. Either of these hypotheses can account for some but not all aspects of vascular pattern formation and are far from being verified as yet (Nelson and Dengler, 1997).

For the purpose of identifying mechanisms responsible for spatial regulation of vascular tissue formation, genetic analysis, which has played an increasingly important role in recent studies of plant development, would be the most promising approach. In *Arabidopsis*, several kinds of mutants showing aberrant vascular formation have been reported. In the *monopteros* mutant, leaf marginal veins are missing or interrupted (Berleth and Jürgens, 1993). In the *gnom* mutant, tracheary elements are not interconnected to form strands but arranged in clusters or as single cells (Jürgens et al., 1991; Mayer et al., 1993). In the *fackel* and the *fass* mutants, lateral veins of the cotyledon are interrupted (Torres Ruitz and Jürgens, 1994; Mayer et al., 1991). These four mutants were identified originally as being impaired in body organization of the seedling. Such morphological abnormalities were traced back to altered embryogenesis. Thus, it is possible that the aberrant venation in these mutants may not be the primary effects of mutations but the secondary effects caused by disorganized body plan. The *lop1* mutant, which is defective in basipetal transport of auxin, also exhibits abnormalities in vascular patterning. The leaves of this mutant are narrowed with a bifurcated and twisted midvein (Carland and McHale, 1996). The *monopteros* mutant was reported to have a reduced capacity of polar transport of auxin (Przemek et al., 1996). Although these findings appear to be consistent with the canalization hypothesis, it is not clear whether the reduced

capacity of auxin transport is the cause or the consequence of the vascular pattern abnormalities.

Mutants of *Arabidopsis* with truly primary defects in vascular formation would be powerful tools for elucidating the molecular basis of the spatial regulation of vascular differentiation. Our strategy for isolating such mutants was to examine vein patterning in the cotyledon for every seedling from each of mutagenized populations of *Arabidopsis* and to select mutant lines of seedlings exhibiting relatively normal appearance and distinct abnormalities in venation of the cotyledon. The successful application of a similar procedure to isolate *Arabidopsis* mutants with venation-specific defects, *cvp1* and *cvp2* was recently reported (Carland et al., 1999). We have screened 3,400 $M_3$ lines which has led to the identification of 12 mutants that are impaired in vascular pattern formation. We briefly describe the characterization of 8 of them (*van1*, *2*, *3*, *4*, *5-1*, *5-2*, *6* and *7*) as a first step of genetic analysis on the spatial control of vascular tissue differentiation and discuss the two possible hypotheses for this, based on the phenotypes of the *van* mutants.

## MATERIALS AND METHODS

### Isolation of mutants

Plants used in the present study were derived from the Landsberg *erecta* (L*er*) strain of *Arabidopsis thaliana* unless otherwise indicated. L*er* is referred to as the wild type in this paper. Wild-type L*er* seeds were mutagenized by treatment with 0.3% ethyl methane sulphonate solution for 20 hours at room temperature. After two cycles of self-fertilization, $M_3$ seeds were collected from individual $M_2$ plants for construction of $M_3$ lines. Each $M_3$ line consists of seeds harvested from only a single $M_2$ plant. Screening was carried out with some of seeds from each $M_3$ line. The $M_3$ seeds were germinated by incubation in water at 22°C for 7 days under continuous white light (30-50 μmol/$m^2$/second). After the resultant seedlings were decolored in 99% ethanol and stained with 1% phloroglucinol in 20% hydrochloric acid, the vessels of the cotyledons were examined under a microscope. $M_3$ lines in which some seedlings exhibited aberrant patterning of the vascular system were selected as mutant lines.

### Linkage analysis

L*er* plants heterozygous for one of *van* mutations were crossed with wild-type Col plants. Seeds were collected from self-pollinated $F_1$ plants heterozygous for the *van* mutation, yielding a polymorphic $F_2$ population. The genotype of the *VAN* locus and simple sequence length polymorphism (SSLP) loci or cleaved amplified polymorphic sequence (CAPS) loci were determined for each individual $F_2$ plant using its $F_3$ progeny. For SSLP and CAPS analysis, DNA was isolated from each family of $F_3$ plants with the IsoPlant Kit (Nippon Gene Co., Tokyo, JAPAN). Polymerase chain reaction (PCR) was performed with a thermal cycler (Gene Amp PCR system 9700, PE Applied Biosystems) by repeating 40 times the following reaction: heat-denaturation at 94°C for 30 seconds, annealing at 55°C for 30 seconds, and polymerization at 72°C for 1 minute. PCR products were resolved by electrophoresis on a Nusieve 3:1 agarose gel (FMC Bioproducts, Rockland, Maine, USA) and recombination frequencies between *VAN* loci and SSLP or CAPS loci were scored.

### Histological analysis

Detailed histological analysis was performed for *van* mutants purified genetically through repeating back crosses three times. In the case of analysis on the vascular tissues of cotyledons, hypocotyls and root tips, seedlings that had been incubated in water for 7 days after seed imbibition were used as the source materials. For analysis of rosette leaves, 20-day-old or 26-day-old plants grown aseptically on germination medium were used. The germination medium was prepared as described by Valvekens et al. (1988) but solidified with 0.25% gellan gum instead of 0.8% agar. All cultures were carried out at 22°C under continuous white light (30-50 μmol/$m^2$/second).

For whole-mount observation, samples were fixed overnight in a 9:1 mixture of ethanol and acetic acid or FAA (a 2.5:2.5:45:50 mixture of formalin, acetic acid, ethanol, and water) at room temperature. Fixed samples were cleared in a mixture of chloral hydrate, glycerol, and water solution (8 g:1 ml:2 ml) and observed under a light microscope equipped with a Nomarski optics (U-DICT; Olympus) or a stereoscopic microscope.

Cross sections of 4 μm thickness were made from hypocotyl samples that had been fixed in FAA, dehydrated in a graded ethanol series, and embedded in the Technovit 7100 resin (Heraeus Kulzer, Germany). These sections were stained with toluidine blue and observed under a light microscope.

### Histochemical localization of GUS activity

Transgenic *Arabidopsis* (Wassilewskija strain), which carried a chimeric gene, *pAthb8*::*GUS*, consisting of the *Athb-8* promoter and the β-glucuronidase (GUS) structural gene (Baima et al., 1995) or a chimeric gene, *pTED3::GUS*, consisting of the *TED3* promoter and the GUS structural gene (Igarashi et al., 1998), was used to distinguish vascular tissues. Seeds of transgenic *Arabidopsis* carrying *pAthb8::GUS* were kindly provided by Dr Baima and Dr Morelli, Unità di Nutrizione Sperimentale.

The *van3* mutation was introduced into the *pAthb8*::*GUS* transgenic plants and *pTED3*::*GUS* transgenic plants by artificial crossing between heterozygous *van3* plants and the transgenic plants. Histochemical GUS staining was performed with seedlings of the $F_2$ generation or embryos of the $F_3$ generation. Samples were fixed in 90% (v/v) acetone for longer than 45 minutes at –20°C. After washing in 100 mM sodium phosphate buffer pH 7.2 at least 3 times, they were immersed in a reaction mixture containing 1 mM 5-bromo-4-chloro-3-indolyl glucuronide, 0.5 mM potassium ferricyanide, and 0.5 mM potassium ferrocyanide in 100 mM sodium phosphate buffer pH 7.2 and incubated at 37°C for 2 hours (*pAthb8::GUS*) or 24 hours (*pTED3::GUS*) in the dark. After the reaction, samples were mounted with a mixture of chloral hydrate, glycerol, and water and observed under a light microscope equipped with a Nomarski optics.

## RESULTS

### Isolation of mutants defective for vascular pattern formation

The cotyledon of *Arabidopsis* has a very simple vein pattern; one midvein and three or four lateral veins (Fig. 1A). Taking this pattern as an index, the mutagenized population was examined for mutants impaired in vascular pattern formation. Screening of 3,400 $M_3$ lines resulted in the isolation of 12 mutant lines, which were characterized by fragmentary lateral veins. Of these, 8 mutant lines (L1315, L1727, L3302, L3409, L3992, L4622, L4668 and L4503) were subjected to further analysis.

### Genetic analysis

In each of mutant $M_3$ lines, approximately a quarter of seedlings exhibited aberrancy in the vascular pattern of the cotyledon and three quarters appeared normal. Self-pollination of two thirds of those normal plants yielded both normal and abnormal progeny at a segregation ratio of 3 to 1 in the next generation ($M_4$). These results indicated that alteration of the

**Table 1. Linkage analysis of *van* mutations**

| Locus | Marker (map position*) | Chromosomes‡ NR | R |
|---|---|---|---|
| *VAN1* | nga1145 (2: 9.60) | 32 | 8 |
| | RNSI (2: 14.59) | 33 | 7 |
| *VAN2* | nga151 (5: 29.62) | 38 | 0 |
| | nga106 (5: 33.35) | 37 | 1 |
| *VAN3* | RCI1B (5: 25.32) | 247 | 3 |
| | nga151 (5: 29.62) | 233 | 3 |
| *VAN4* | CTR1 (5: 9.32) | 35 | 5 |
| | nga225 (5: 14.31) | 34 | 8 |
| *VAN5* | nga63 (1: 11.48) | 84 | 4 |
| | f15571 (1: 26.29) | 70 | 6 |
| *VAN6* | nga12 (4: 22.92) | 32 | 0 |
| | nga8 (4: 26.56) | 33 | 1 |
| *VAN7* | NCC1 (1: 12.60) | 89 | 11 |
| | f15571 (1: 26.29) | 79 | 3 |

*Chromosome number and map position on the recombinant inbred map (http://nasc.nott.ac.uk/).

‡The number of nonrecombinant (NR) or recominant (R) chromosomes scored at the marker position.

vascular pattern was caused by a monogenic, recessive mutation in each mutant line.

To determine the number of complementation groups, heterozygous plants belonging to different mutant lines were crossed to each other. Any cross among L1315, L1727, L3302, L3409, L3992, L4668 and L4503 resulted in recovery from mutant phenotype in all $F_1$ seedlings, indicating that mutations in these lines were located at different loci (data not shown). Only a cross between L3992 and L4622 brought about segregation of wild-type and mutant phenotypes, the ratio of which did not deviate significantly from 3:1 (data not shown). Since L3992 and L4622 were derived from different batches of $M_1$ plants, they should not be the re-isolated lines of the same mutant but the allelic lines. Thus, these 8 mutant lines were found to represent single mutant alleles at 6 genetic loci and two mutant alleles at one locus. In view of the characteristics of the mutations that affected vascular network, the genes defined by mutations in L1315, L1727, L3302, L3409, L3992/L4622, L4668 and L4503 were designated *VAN1*, *VAN2*, *VAN3*, *VAN4*, *VAN5*, *VAN6* and *VAN7*, respectively. Mutant alleles of L3992 and L4622 were designated *van5-1* and *van5-2* for distinguishing them.

## Linkage analysis

Table 1 summarizes the result of linkage analysis, which localized *VAN1*, *VAN2*, *VAN3*, *VAN4*, *VAN5*, *VAN6* and *VAN7* loci on chromosomes 2, 5, 5, 5, 1, 4 and 1, respectively. Comparison of these *VAN* loci with genetic loci, mutants of which have been shown to affect vascular patterns, suggested possible relationship between *VAN5* and *MONOPTEROS* and between *VAN7* and *EMB30/GNOM*. Complementation analysis revealed that *van7* is allelic to *emb30/gnom* while *van5* is not allelic to *monopteros* (data not shown). Thus, *van7* was renamed *emb30-7* as a new mutant allele of *EMB30/GNOM*. Carland et al. (1999) reported that *CVP1*, one of newly identified loci participating in vein pattern formation, was located between molecular markers of m235 and m59 in chromosome 1. Reference of *van5* to this locus is to be tested.

## Vein patterns of *van* mutants

Vascular patterns in the cotyledons of 7-day-old seedlings of the *van* mutants are shown in Fig. 1B-I. Although the vascular patterns of the *van1*, *van2*, *van3*, *van4* and *van6* mutants appeared similar to the wild-type pattern in their overall architecture, the lateral veins of these mutants were incomplete and disconnected (Fig. 1B,C,D,E,H). Fragmentation of lateral vein was most noticeable in the *van3* mutant (Fig. 1D). The architecture of the venation of the *van5* mutant was rather different from that of the wild type, and highly variable among the *van5* individuals (Fig. 1F,G). Lateral veins were not obvious in the cotyledon of the *emb30-7* (*van7*) mutant and many tracheary elements were arranged randomly in its central region (Fig. 1I). An additional feature of the vascular tissue shared by all the *van* mutants was that tracheary elements were very large as compared with normal tracheary elements in the wild type. In spite of the noticeable abnormalities in the vascular pattern, cotyledons of the *van1*, *van2*, *van3*, *van4* and *van6* mutants appeared normal in shape. Cotyledons of the *van5-1* and *van5-2* mutants were distorted and much smaller than those of the wild type. The *emb30-7* cotyledon was apparently circular.

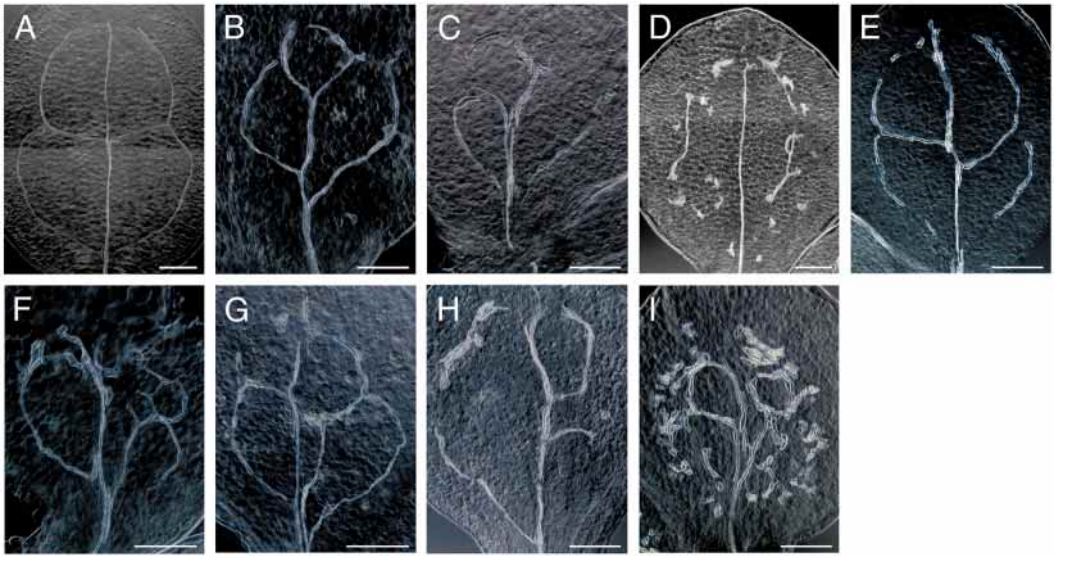


**Fig. 1.** Vascular patterns in cotyledons of wild-type (A) and *van* mutant (B-I) seedlings incubated for 7 days. (B) *van1*. (C) *van2*. (D) *van3*. (E) *van4*. (F) *van5-1*. (G) *van5-2*. (H) *van6*. (I) *emb30-7* (*van7*). The scale bars represent 100 μm.

Fig. 2 shows the vascular tissues of rosette leaves in adult plants of the wild type and *van* mutants other than *van1*, which did not expand rosette leaves. The first rosette leaf of the wild type has a prominent midvein (primary vein), secondary veins which branch from the primary vein, and tertiary veins which branch from the secondary veins (Fig. 2A). In the first rosette leaves of the *van2* through *van6* mutants, tertiary veins were absent, faint, or fragmentary whereas primary and secondary veins formed a fairly continuous network (Fig. 2B-G). The primary and secondary veins of the *van5* mutant consisted of a greater number of tracheary elements (per unit length) than the wild-type veins (Fig. 2E,F). The extra tracheary elements were aligned improperly in the *van5* veins. In the case of the *emb30-7* mutant, rosette leaves had three-dimensional and complex networks of the vascular system with an increasing number of free ends (Fig. 2H). This phenotype was most obvious in the peripheral zone of the leaf lamia.

All of these *van* mutations induced a reduction in size of the rosette leaf lamina. In addition to this effect, the *van5* and *emb30-7* mutations caused remarkable alterations in the overall morphology of the rosette leaves. *van5* distorted leaf shape (Fig. 2E,F) and *emb30-7* increased the thickness of leaves.

## Morphology of *van* mutants at the whole-plant level

Young seedlings of the *van* mutants are shown in Fig. 3. The most apparent abnormality in morphology at the whole-plant level was poor growth of the primary root in all of the *van* mutants. In other aspects such as cotyledon expansion, greening, and hypocotyl elongation, all the *van* mutants exhibited relatively normal appearances. However, closer observation revealed various effects of the *van* mutations on the shape and size of cotyledons, as described in the previous paragraph.

At the later stages of development, all the *van* mutations caused more severe effects on plant morphology and growth. The degree of morphological abnormality of 20-day-old mutant plants increased in the order of *van3* < *emb30-7* (*van7*) < *van4* < *van2*, *van5-1*, *van5-2*, *van6* < *van1* (Fig. 4). The *van1* plant showing the most severe phenotype formed only two visible rosette leaves, which did not expand (Fig. 4B). The *van3* plant showing the slightest phenotype developed more than 7 rosette leaves of almost normal shape though they were significantly smaller than the wild-type leaves (Fig. 4D). The *van* mutants died after several weeks of vegetative growth and bolting was never observed in any of them.

## Vascular systems along the main axes of *van* mutants

Vascular systems of the hypocotyl (Fig. 5) and root (Fig. 6) were examined in wild-type and *van* seedlings grown for 7 days. Microscopic observation of cleared, whole-mount specimens of hypocotyls could not detect obvious differences in the longitudinal alignments of vessels between wild type (Fig. 5A) and *van1* through *van6* mutants (Fig. 5B-H). In the majority of the *emb30-7* seedlings, the apical ends of some vessels were found in the middle part of the hypocotyl (Fig. 5I).

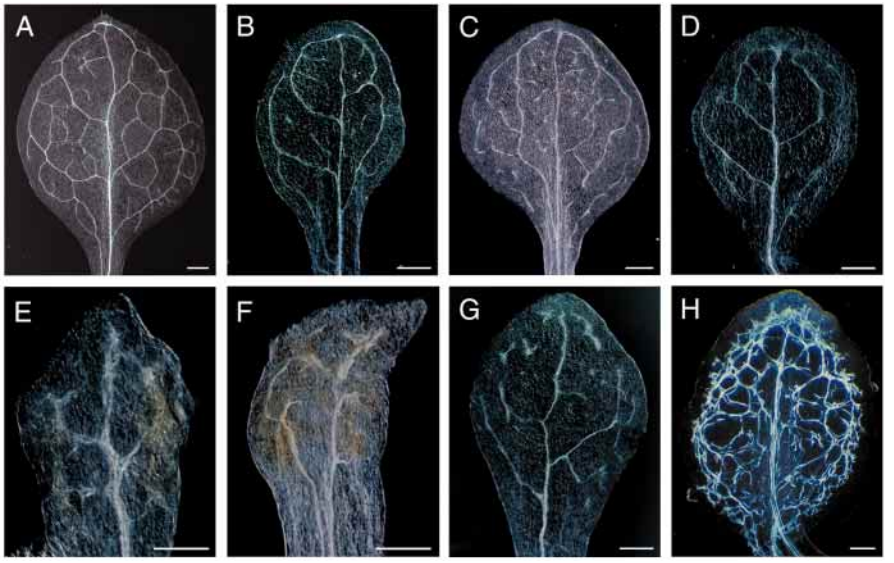


**Fig. 2.** Vascular patterns in the first rosette leaves of wild-type (A) and *van* mutant (B-H) plants grown for 20 to 26 days. (B) *van2*. (C) *van3*. (D) *van4*. (E) *van5-1*. (F) *van5-2*. (G) *van6*. (H) *emb30-7* (*van7*). The scale bars represent 500 μm.


**Fig. 3.** Morphology of 7-day-old seedlings of the wild type (A) and *van* mutants (B-I). (B) *van1*. (C) *van2*. (D) *van3*. (E) *van4*. (F) *van5-1*. (G) *van5-2*. (H) *van6*. (I) *emb30-7* (*van7*). The scale bars represent 500 μm.

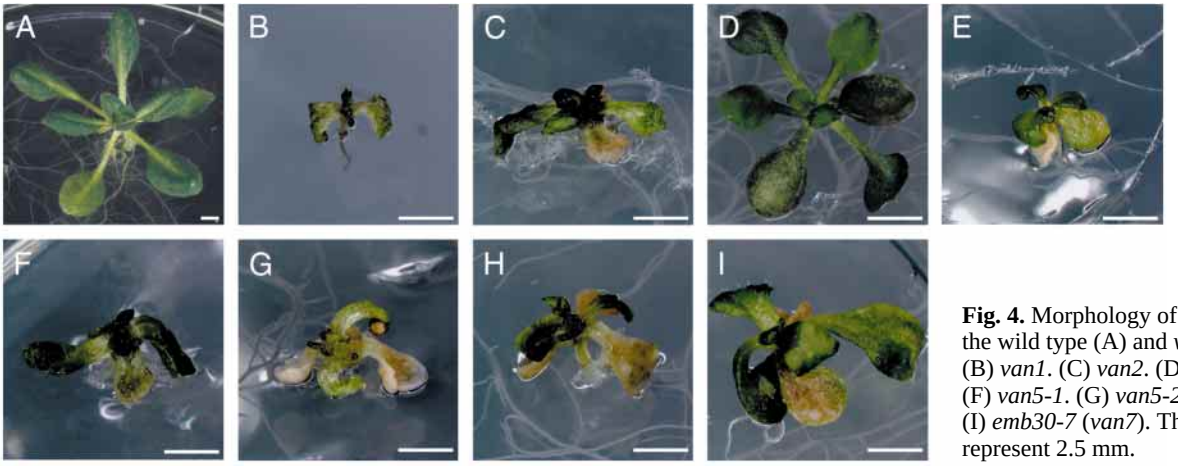


**Fig. 4.** Morphology of 20-day-old plants of the wild type (A) and *van* mutants (B-I). (B) *van1*. (C) *van2*. (D) *van3*. (E) *van4*. (F) *van5-1*. (G) *van5-2*. (H) *van6*. (I) *emb30-7* (*van7*). The scale bars represent 2.5 mm.

Vascular tissues of the hypocotyl were also examined anatomically with transverse sections, which detected some aberrancies of vascular organization in every *van* mutant except *van3* (Fig. 5J-R). In the *van1* mutant, radial arrangement of cells in the central cylinder was strikingly disordered, and phloem could hardly be identified (Fig. 5K). Such tendency was observed in the *van2*, *van4*, *van5-1*, *van5-2*, and *van6* mutants (Fig. 5L,N-Q) although their phenotypes were less severe as compared with the *van1* (Fig. 5K). In the *emb30-7* hypocotyls, lack of one strand of phloem was sometimes observed but otherwise radial organization of vascular cells looked normal (Fig. 5R).

In the primary roots of the *van* mutants other than the *van1*, the meristematic zone was reduced in length, and vessel differentiation took place at the position unusually close to the root apex (Fig. 6C-I). With respect to the continuity of vascular strands, however, these mutant roots appeared to be intact. Obvious defects in the root vascular system were observed only in the *van1* mutant, where vessels were disconnected and/or improperly aligned (Fig. 6B).

## Vascular differentiation during late embryogenesis of *van3* mutant

Further experiments were performed with a predominant focus on the *van3* mutation, which showed the most restricted effect among *van* mutations. To decide steps of the vascular tissue

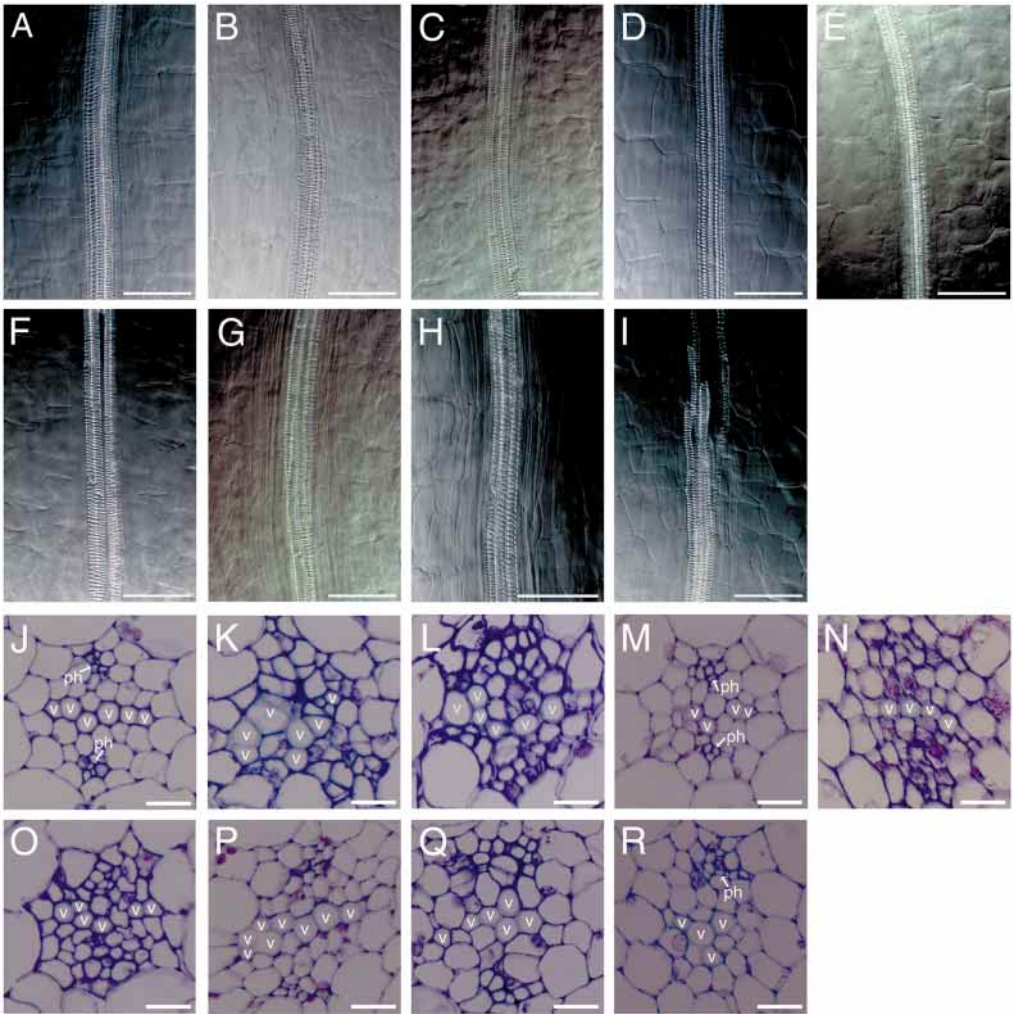


**Fig. 5.** Vascular bundles in the hypocotyls of the wild-type (A,J) and *van* mutant (B-I, K-R) seedlings incubated for 7 days. (B,K) *van1*. (C,L) *van2*. (D,M) *van3*. (E,N) *van4*. (F,O) *van5-1*. (G, P) *van5-2*. (H,Q) *van6*. (I,R) *emb30-7* (*van7*). (A-I) Whole-mount of the central part of the hypocotyls. (J-R) Transverse sections of the basal part of the hypocotyls. Vessels (v) and phloems (ph) are indicated in each photograph. The scale bars represent 50 μm (A-I) and 10 μm (J-R).

differentiation that are affected by the *van3* mutation, the expression patterns of *pAthb8::GUS* and *pTED3::GUS* chimeric genes were examined as molecular markers under the influence of the *van3* mutation. As the *pAthb8::GUS* and *pTED3::GUS* genes are expressed preferentially in the provascular/vascular tissues (Baima et al., 1995) and differentiating tracheary elements (Igarashi et al., 1998), respectively, their expression patterns can distinguish provascular tissue differentiation and tracheary element differentiation. In the cotyledon of the walking-stick stage embryo of the wild type, *pAthb8::GUS*-expressing cells were aligned in the 'ϕ'-letter shape, which corresponded to a midvein and a distal loop of lateral veins (Fig. 7A). At the upturned-U stage, *pAthb8::GUS*-expressing cells appeared in the basal part of the lateral veins to complete a circuit of provascular tissues (Fig. 7B). In contrast, *pAthb8::GUS*-expressing cells of the *van3* cotyledon did not form continuous lateral loops at any stage of late embryogenesis (Fig. 7E,F) or at the young-seedling stage (Fig. 7G) although the overall tendency of GUS expression, initiating at the distal part and reaching to the basal part, was similar to that of the wild type (Fig. 7A-C). Expression of *pTED3::GUS* was not detectable in either the wild-type or the *van3* cotyledon during embryogenesis (data not shown). In the cotyledons of 7-day-old wild-type seedlings, *pTED3::GUS* was specifically expressed in immature tracheary elements and tracheary element precursor cells of the midvein and lateral veins (Fig. 7D). This was also the case for the *van3* mutant, and no GUS-expressing cells were observed in the interspace between the fragmented lateral veins (Fig. 7H). These results indicated that the *van3* mutation affected very early aspects of vascular patterning prior to provascular network formation without interfering with progression of the vascular tissue differentiation.

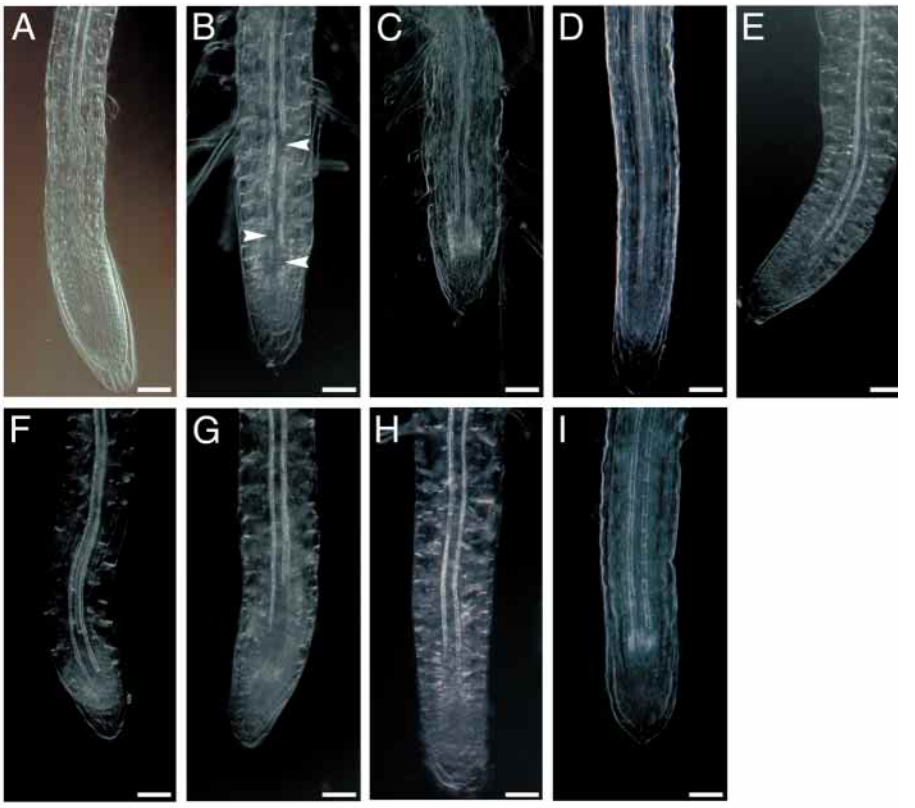


**Fig. 6.** Xylem strands in the root of the wild-type (A) and *van* mutant (B-I) seedlings incubated for 7 days. (B) *van1*. (C) *van2*. (D) *van3*. (E) *van4*. (F) *van5-1*. (G) *van5-2*. (H) *van6*. (I) *emb30-7* (*van7*). Arrowheads indicate discontinuity points of vessels. The scale bars represent 50 μm.

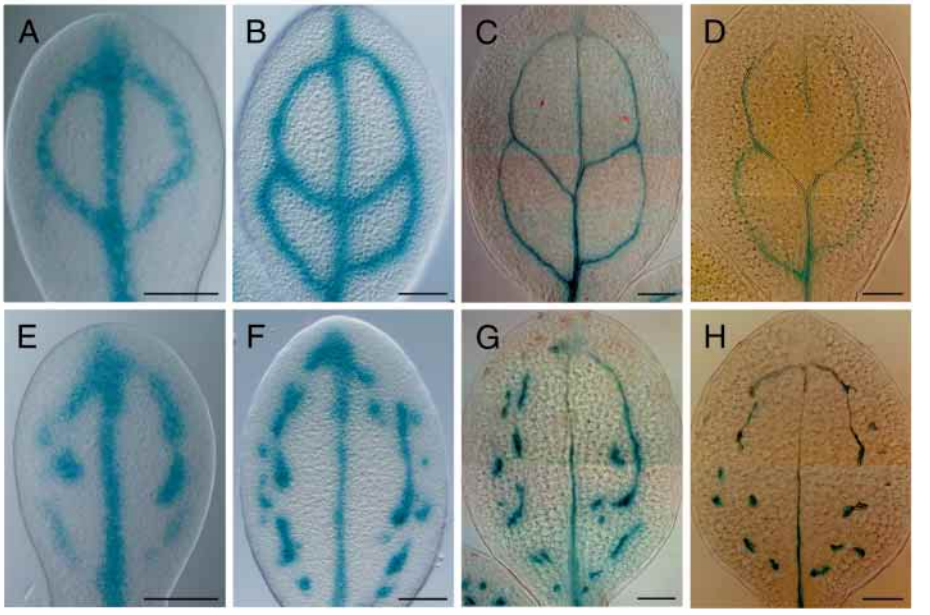


**Fig. 7.** Histochemical localization of GUS activity in the wild type (A-D) and *van3* mutant (E-H) carrying the *pAthb8*::*GUS* gene (A-C, E-G) or the *pTED3*::*GUS* gene (D,H). (A,E) Cotyledon of the walking-stick stage embryo. (B,F) Cotyledon of the upturned-U stage embryo. (C,D,G,H) Cotyledon of the 7-day-old seedlings. The scale bars represent 100 μm.

## DISCUSSION

### Vein patterns of *van* mutants

In the present study, we screened mutagenized populations of *Arabidopsis* with the aim of isolating vascular patterning mutants as genetic tools for studying regulatory mechanisms of vascular tissue differentiation. Screening of 3,400 M3 lines with the cotyledonary

venation as a guide allowed us to identify 7 genetic loci (*VAN1* through *VAN7*) that are involved in the vascular network formation. Mutations in these *VAN* loci caused severe defects in minor veins such as lateral veins of the cotyledon and tertiary veins of the rosette leaf while they were less injurious to major veins including midveins of the cotyledon and the rosette leaf. These phenotypes suggest that both the machinery controlling lateral vein formation in the cotyledon and the machinery controlling tertiary vein formation in the rosette leaf involve *VAN* gene products as common components. In addition, it can be inferred from the *van* phenotypes that major and minor vasculatures are formed under different genetic controls. This does not necessarily indicate difference in the fundamentals of the regulatory systems but may represent difference in the robustness of the similar systems.

Among the *van* mutants, *emb30-7* (*van7*) is distinct from the *van1* through *van6* in several aspects of venation. In contrast to the cotyledons of most of the *van* mutants, in which lateral veins were incomplete or fragmented but still present in relatively normal architecture (Fig. 1B-E,H), the *emb30-7* cotyledon lost lateral veins and had clustered tracheary elements instead (Fig. 1I). This phenotype of the *emb30-7* is almost the same as reported for the *gnom* mutant (Jürgens et al., 1991), which is allelic to *emb30*. The rosette leaves of the *van2* through *van6* mutants had simplified venation with fragmentation or (partial) loss of tertiary veins in the rosette leaf (Fig. 2B-G) whereas the *emb30-7* rosette leaf had rather complicated venation with an increasing number of freely ending veinlets, particularly near the periphery (Fig. 2H). Such venation of the *emb30-7* rosette leaf appears similar to the venation observed for *Arabidopsis* seedlings that were incubated in the presence of inhibitors of auxin polar transport (Mattsson et al., 1999). The *EMB30*/*GNOM* gene encodes a Sec7-like protein, which may be involved in vesicle trafficking (Shevell et al., 1994; Busch et al., 1996). Recently, the *gnom* mutation was found to interfere with localization of an auxin efflux carrier, PIN1 (Steinmann et al., 1999). Taken together, we can reasonably speculate that the aberrant venation of the *emb30-7* mutant may be induced by the reduction in auxin polar transport due to defects in vesicle trafficking and the resultant irregularity in the PIN1 localization.

### Effects of *van* mutations on various aspects of seedling development

Noticeable characters other than fragmentary venations common to young seedlings of all the *van* mutants were poor growth of the primary root (Fig. 3) and reduction in the size of root apical meristem (Fig. 6). This suggests that high meristematic activity of the primary root is linked with integrity of a vein network in the cotyledon in some way. However, this linkage is unlikely to be a simple and direct, considering that root growth and development of *cvp1* and *cvp2* mutants defective in the cotyledonary venation were indistinguishable from those of the wild type (Carland et al., 1999).

Microscopic examination of vascular tissues along the hypocotyl-root axis with young seedlings of the *van* mutants discovered additional effects of the *van* mutations particularly on a radial pattern of vascular tissues. In this respect, only the *van3* mutant was normal, and all other *van* mutants exhibited some aberrancies. As the degree of such aberrancies appeared in almost parallel with the degree of morphological defects of the mutant plants, one can suppose that disorganization of vascular tissues along the main axis has a greater influence on development and growth at the whole-plant level than fragmentation of lateral veins in the cotyledon does.

### Involvement of *VAN3* gene in provascular development

The *van3* mutation seems to affect primarily and specifically vascular patterning of the minor veins since the *van3* seedling was almost normal in other morphological aspects including the size and shape of the cotyledon, longitudinal alignment of vessels along the main axis, and radial organization of vascular tissues in the hypocotyl (Figs 1D, 2C, 3D, 4D, 5D, 5M, 6D). Closer characterization of the *van3* mutant throughout embryogenesis, using *pTED3::GUS* and *pAthb8::GUS* expressions as indices of vascular tissue differentiation, detected the discontinuity in the provascular tissues of the lateral vein in the cotyledon at the walking-stick stage (Fig. 7E). Accordingly, the *VAN3* gene is expected to play an important role in the spatial control of provascular differentiation, which results in a continuous network of vascular strands.

Recently isolated mutants of *Arabidopsis*, *cvp1* and *cvp2*, are characterized by a defect specific to the formation of lateral loops of the cotyledonary veins (Carland et al., 1999). This phenotype was shown to be traced back to the incomplete network of provascular tissues. In this regard, the *cvp* mutants are very similar to the *van3* mutant. Functional relationships among the *CVP1*, *CVP2* and *VAN3* genes would be of great interest in the future analysis of provascular tissue patterning.

### Auxin signal flow canalization hypothesis versus diffusion-reaction prepattern hypothesis

With respect to the possible mechanisms determining vein patterns, two hypotheses, i.e., auxin signal flow canalization and diffusion-reaction prepattern, have been proposed and discussed. Mattsson et al. (1999) examined the effects of inhibitors of auxin polar transport on the venation of *Arabidopsis* and attempted to explain the inhibitor-induced alterations in the venation on the basis of the canalization hypothesis. Przemeck et al. (1996) reported a reduced capacity of auxin polar transport and aberrant vasculatures in *monopteros* mutant of *Arabidopsis*, and discussed these features of *monopteros* in reference to the canalization hypothesis. Mutations in the *EMB30/GNOM* locus may also influence venation via suppression of auxin polar transport, as discussed above. These studies, together with pioneering works of Sachs (1968, 1969, 1975), seem to support strongly the canalization hypothesis. Strictly speaking, however, any findings reported so far are not really supportive but rather neutral for the following reasons.

(i) The auxin signal flow canalization hypothesis presumes that positive-feedback regulation of auxin polar transport and the resultant formation of canal networks conducting auxin flow direct the positions of vascular tissue differentiation. These core assumptions have not been verified through recent studies.

(ii) Indispensability of auxin polar transport in normal development of vasculatures, which has been demonstrated by recent studies, can be explained in various ways without assuming the canalization hypothesis, and is not contradictory at all to the diffusion-reaction prepattern hypothesis.

(iii) Abnormalities in vascular development undoubtedly influence auxin polar transport since vascular parenchyma takes a major part in auxin polar transport. Thus, poor ability of auxin

polar transport in mutants with aberrant vascular patterning may not always be the cause of abnormal development of the vascular system but the result of it in some cases.

Most of the *van* mutants formed discontinuous networks of the minor veins but maintained relatively normal architecture of venation as a whole. High frequency of these *van* mutants in the mutagenized population suggests that the continuity of the vein networks is more sensitive to genetic lesions than their overall architecture is. This nature of pattern formation of minor veins is very important when considering the validity of the two hypothetical mechanisms.

A basic model of diffusion-reaction systems hypothesizes interacting substances with different diffusion rates, which can generate stable patterns autonomously in the initially homogenous field through local autocatalysis and long-range inhibition. Meinhardt (1989, 1995) demonstrated that slight changes of this autocatalytic condition readily induced a gradual shift from stripe pattern to spotted pattern via fragmented stripe pattern without destroying the overall architecture. In addition, various alterations of the rate of the basal synthesis, decay, or interaction of the diffusion-reaction substance(s) were also shown to change a pattern from stripes to spots (Asai et al., 1999). In view of such fragility of the continuous patterns developed by diffusion-reaction systems, it is not surprising that the networks of minor veins were fragmented by so many mutations, given that they are controlled on the basis of a version of diffusion-reaction systems as assumed by the diffusion-reaction prepattern hypothesis.

In the vein pattern formation predicted by the canalization hypothesis, in contrast, the overall architecture of the vascular network is supposed to be more fragile than its continuity. The canalization hypothesis assumes that auxin flow builds a canal for conducting auxin flow by itself without any blueprints and that this canal produces a pattern of vasculature. Therefore, all mutations that interfere with auxin flow or canal formation thus preventing continuous formation of vascular networks should necessarily destroy the overall architecture of the vascular pattern. This is apparently not consistent with the discontinuous network of the minor veins with relatively normal architecture found in the *van* mutants. Thus, the *van* mutants seem to support the diffusion-reaction hypothesis rather than the canalization hypothesis.

The above argument based on the phenotypes of the *van* mutants calls the canalization hypothesis into question and indicates that the diffusion-reaction hypothesis still survives as a candidate for a mechanism determining vascular patterns, in particular, minor venations. Isolation and molecular characterization of the *VAN* genes would provide important information about how vascular tissues are differentiated continuously to form networks and whether the canalization mechanism or the diffusion-reaction mechanism is responsible for vein pattern formation.

We thank Dr Baima and Dr Morelli, the Unità di Nutrizione Sperimentale, for providing transgenic *Arabidopsis* seeds carrying *pAthb8::GUS*, Dr Berleth, the University of Toronto, for providing *monopteros* seeds, and the Arabidopsis Biological Resource Center (Columbus, Ohio, USA) for providing *gnom* seeds. We also thank Miss Matsuda and Miss Furumizu, University of Tokyo, for their help in linkage analysis. This work was supported in part by Grants-in-Aid from the Ministry of Education, Science, Sports and Culture of Japan (No. 10304063, No. 10219201, No. 10182101), and from the Japan Society for the Promotion of Science (JSPS-RFTF96L00605) to H. F.

## REFERENCES

**Asai, R., Taguchi, E., Kume, Y., Saito, M. and Kondo, S.** (1999). Zebrafish *Leopard* gene as a component of the putative reaction-diffusion system. *Mech. Dev.* **89**, 87-92.

**Baima, S., Nobili, F., Sessa, G., Lucchetti, S., Ruberti, I. and Morelli, G.** (1995). The expression of the *Athb-8* homeobox gene is restricted to provascualr cells in *Arabidopsis thaliana*. *Development* **121**, 4171-4182.

**Berleth, T. and Jürgens, G.** (1993). The role of the *monopteros* gene in organising the basal body region of the *Arabidopsis* embryo. *Development* **118**, 575-587.

**Busch, M., Mayer, U. and Jürgens, G.** (1996). Molecular analysis of the *Arabidopsis* pattern formation gene *GNOM*: gene structure and intragenic complementation. *Mol. Gen. Genet.* **250**, 681-691.

**Carland, F. M. and McHale, N. A.** (1996). *LOP1*: a gene involved in auxin transport and vascular patterning in *Arabidopsis*. *Development* **122**, 1811-1819.

**Carland, F. M., Berg, B. L., FitzGerald, J. N., Jinamornphongs, S., Nelson, T. and Keith, B.** (1999). Genetic regulation of vascular tissue patterning in arabidopsis. *Plant Cell* **11**, 2123-2137

**Igarashi, M., Demura, T. and Fukuda, H.** (1998). Expression of the *Zinnia TED3* promoter in developing tracheary elements of transgenic *Arabidopsis*. *Plant Mol. Biol.* **36**, 917-927.

**Jürgens, G., Mayer, U., Torres Ruiz, R. A., Berleth, T. and Miséra, S.** (1991). Genetic analysis of pattern formation in the *Arabidopsis* embryo. *Development* **Supplement 1**, 27-38.

**Koch, A. J. and Meinhardt, H.** (1994). Biological pattern formation: from basic mechanisms to complex structures. *Rev. Mod. Phys.* **66**, 1481-1507.

**Mattsson, J., Sung, Z. R. and Berleth, T.** (1999). Responses of plant vascular systems to auxin transport inhibition. *Development* **126**, 2979-2991.

**Mayer, U., Büttner, G. and Jürgens, G.** (1993). Apical-basal pattern formation in the *Arabidopsis* embryo: studies on the role of the *gnom* gene. *Development* **117**, 149-162.

**Mayer, U., Torres Ruiz, R. A., Berleth, T., Miséra, S. and Jürgens, G.** (1991). Mutations affecting body organization in the *Arabidopsis* embryo. *Nature* **353**, 402-407.

**Meinhardt, H.** (1982). *Models of Biological Pattern Formation.* London: Academic Press.

**Meinhardt, H.** (1989). Models for positional signalling with application to the dorsoventral patterning of insects and segregation into different cell types. *Development* **Supplement**, 169-180.

**Meinhardt, H.** (1995). Dynamics of stripe formation. *Nature* **376**, 722-723.

**Nelson, T. and Dengler, N.** (1997). Leaf vascular pattern formation. *Plant Cell* **9**, 1121-1135.

**Przemeck, G. K. H., Mattsson, J., Hardtke, C. S., Sung, Z. R. and Berleth, T.** (1996). Studies on the role of the *Arabidopsis* gene *MONOPTEROS* in vascular development and plant cell axialization. *Planta* **200**, 229-237.

**Sachs, T.** (1968). The role of the root in the induction of xylem differentiation in peas. *Ann. Bot.* **32**, 391-399.

**Sachs, T.** (1969). Polarity and the induction of organized vascular tissues. *Ann. Bot.* **33**, 263-275.

**Sachs, T.** (1975). The control of the differentiation of vascular networks. *Ann. Bot.* **39**, 197-204.

**Sachs, T.** (1989). The development of vascular networks during leaf development. *Curr. Top. Plant Biochem. Physiol.* **8**, 168-183.

**Sachs, T.** (1991). Cell polarity and tissue patterning in plants. *Development* **Supplement 1**, 83-93.

**Shevell, D. E., Leu, W. M., Gillmor, C. S., Xia, G., Feldmann, K. A. and Chua, N. H.** (1994). *EMB30* is essential for normal cell division, cell expansion, and cell adhesion in Arabidopsis and encodes a protein that has similarity to Sec7. *Cell* **77**, 1051-1062.

**Steinmann, T., Geldner, N., Grebe M., Mangold, S., Jackson, C. L., Paris, S, Gälweiler, L., Palme, K. and Jürgens, G.** (1999). Coordinated polar localization of auxin efflux carrier PIN1 by GNOM ARF GEF. *Science* **286**, 316-318.

**Torres Ruiz, R. A. and Jürgens, G.** (1994). Mutations in the *FASS* gene uncouple pattern formation and morphogenesis in *Arabidopsis* development. *Development* **120**, 2967-2978.

**Valvekens, D., Van Montagu, M. and Van Lijsebettens, M.** (1988). *Agrobacterium tumefaciens*-mediated transformation of *Arabidopsis thaliana* root explants by using kanamycin selection. *Proc. Natl. Acad. Sci. USA* **85**, 5536-5540.